# Influence of Bi impurity on the main parameters of the current-voltage characteristics of the $Ge_2Sb_2Te_5$ phase-change memory semiconductor

© S.A. Fefelov[1], L.P. Kazakova[1,2], N.A. Bogoslovskiy[1], A.B. Bylev[2], E.V. Gushchina[1], Zh.K. Tolepov[3], A.S. Zhakypov[3], O.Yu. Prikhodko[3]

[1] Ioffe Institute,
194021 St. Petersburg, Russia
[2] Kirov State Forest Technical University,
194021 St. Petersburg, Russia
[3] Al Farabi Kazakh National University,
050038 Almaty, Kazakhstan

E-mail: s.fefelov@list.ru

*Received April 12, 2024*
*Revised September 19, 2024*
*Accepted October 1, 2024*

The current-voltage characteristics of thin-film samples of the $Ge_2Sb_2Te_5$ phase-change memory material are measured in a current control mode. The influence of Bi impurity on the main parameters of the current-voltage characteristic is studied. The obtained results show an increase in the stability of the electrical properties of $Ge_2Sb_2Te_5$ when doped with Bi at concentrations of 6.3 and 12.0 at%. The introduction of Bi impurity leads to the disappearance of voltage fluctuations after switching.

**Keywords:** chalcogenide glassy semiconductors, $Ge_2Sb_2Te_5$, phase-change memory, bismuth doping.

DOI: 10.61011/SC.2024.08.59891.6261

## 1. Introduction

Comprehensive studies of the properties of a chalcogenide glassy semiconductor (CGS) of the $Ge_2Sb_2Te_5$ composition (GST225), which is considered to be the most promising material for non-volatile memory elements based on the chalcogenide glass–crystal phase transition [1–3], have attracted much attention recently. GST225 is currently being used more and more often in this capacity [4,5]. This makes it important to identify the key mechanisms of conductivity enhancement in strong electric fields that underlie the transition of thin CGS films from a high-resistance state to a low-resistance one (switching effect) and the transition of a sample from an amorphous state to a crystalline one with low resistance (i.e., „memorization" of the low-resistance state, or memory effect). It is also important to find ways to control the main parameters characterizing the memory effect. With this aim in view, we conducted a study of the current–voltage characteristics (CVCs) of undoped GST225 films and the same films doped with bismuth. The Bi impurity was chosen based on the results reported in [6–9], where the introduction of Bi was found to reduce the data recording time, enhance the recording stability, and increase the data retention time, which is relevant to the production of phase-change memory devices. The application of GeSbTe CGSs is not limited to memory elements only. These materials are currently being used actively in optoelectronics and nanophotonics [2,10,11] and in neuromorphic computing [12–14]. Controlled modification of material properties through doping is quite useful in all of these applications.

## 2. Samples and experimental procedure

The studied samples were thin-film sandwich-type CGS structures. Amorphous GST225 films and Bi-doped GST225 films were obtained by ion-plasma RF (13.56 MHz) magnetron sputtering of a composite GST225–Bi target in Ar atmosphere under a pressure of $\sim 1$ Pa. An ONYX-3 magnetron (Angstrom Sciences) with a cooled cathode, a polycrystalline target of the $Ge_2Sb_2Te_5$ composition with a chemical purity of 99.999% (AciAlloys), and Bi targets of the same purity were used in the process. The amorphism of the structure was verified by Raman spectroscopy (Solver Spectrum spectrometer with a He–Ne laser, $\lambda = 633$ nm). The composition of the obtained films was monitored via energy-dispersive analysis using a Quanta 3D 200i scanning electron microscope (SEM). The thickness of these films was determined by scanning the cleaved surface of sandwich structures with the SEM electron beam. The concentration of Bi impurity in the films was 6.3 and 12.0 at%, and their thickness was $\sim 130$ nm.

Amorphous films were deposited onto a Si substrate with conductive TiN coating and onto a glass substrate with conductive Al coating. The conductive coating served as the base electrode in electrical measurements, and gold was used as the top pressure electrode. The area of contact between the film and the top electrode was $\sim 10^{-4}$ cm$^2$. The pressure electrode was shifted along the film surface to perform measurements at different points, which amounts to having a large number of samples.

The measurements were carried out in the current control mode [15]. Triangular current pulses shaped by a digital-to-analog converter were applied to the samples. The rise and

fall times of the current pulse were both equal to 1 ms. A sequence of current pulses with increasing current amplitude $I_{max}$ were applied to the sample. A digital oscilloscope was used to obtain synchronized oscilloscope records of current and voltage at the sample, which were then used to plot the CVCs. This technique allows one to examine in detail the CVCs and the processes accompanying the formation of a state with memory [15–17].

## 3. Experimental results and discussion

Figure 1 shows the oscilloscope records for undoped and doped samples with the base electrode made of TiN (Figure 1, *a*) and Al (Figure 1, *b*). The sharp voltage change (surge) seen in these records corresponds to switching (i. e., transition of the sample from a high-resistance state to a low-resistance one). The maximum voltage in the high-resistance state ($U_{th}$) is called the threshold, or switching, voltage. Following switching, the sample voltage normally remains constant while the current increases significantly. The corresponding voltage is called holding voltage $U_{hold}$. In this case, the total current increases due to expansion of the current filament formed in switching. The temperature within the current filament increases, and crystallization occurs. This is how the formation of a state with memory (i. e., the preservation of a low-resistance state after the removal of external excitation) is interpreted in the electron-thermal switching model [18,19].

The oscilloscope records for undoped samples reveal voltage oscillations after switching, which may be associated with instability of the conducting channel in the CGS film in the process of formation of a state with memory [16]. It follows from Figure 1 that doped samples normally had no voltage fluctuations. This suggests that the crystalline phase is more stable in doped samples, which is apparently attributable to a higher crystal nucleating power of the samples.

Figure 2 presents the typical CVCs obtained for undoped GST225 films and the films with a Bi impurity concentration of 6.3 and 12.0 at% and base electrodes made of TiN (Figure 2, *a*) and Al (Figure 2, *b*). It can be seen that the sample undergoes a jump-like transition from a high-resistance state, which corresponds to the lower CVC branch, to a low-resistance one at voltage $U_{th}$.

In our experiments, a sharp voltage surge (switching effect) was noted only once in both undoped and doped samples. When subsequent current pulses with higher $I_{max}$ values were applied to the samples, a smooth transition to a new lower-resistance state was observed (Figure 3).

The almost complete lack of a vertical CVC section corresponding to holding voltage $U_{hold}$ was an important feature of the samples with a Bi concentration of 12.0 at%.

It can be seen from Figure 2 that, within the section recorded after switching, the reverse branch of the obtained CVCs, which corresponds to a decrease in current applied to the sample, is virtually coincident with the

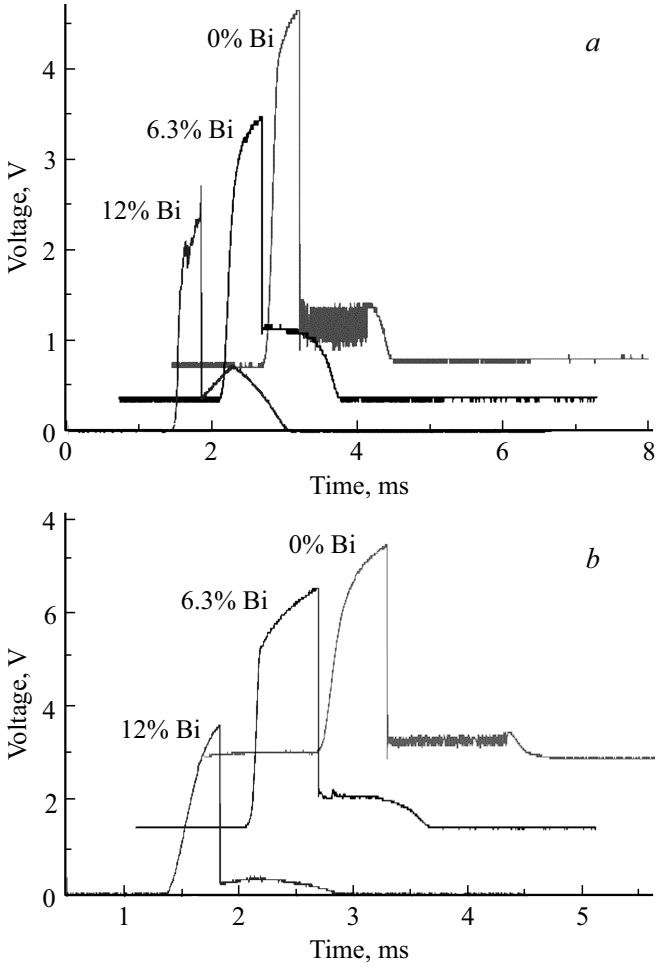


**Figure 1.** Typical oscilloscope records for GST225 samples with TiN (*a*) and Al (*b*) base electrodes at different Bi impurity concentrations. A sharp voltage surge represents switching. The curves corresponding to different concentrations are shifted along both axes for clarity.

forward branch measured with increasing current. The increasing CVC branch plotted for the next current pulse also goes along this section. This fact suggests that crystallization of the sample occurs almost immediately after switching. As a result, the subsequent increase in current does not induce a change in the sample resistance.

Having analyzed the CVCs of the studied samples, we found that the values of switching voltage $U_{th}$ in undoped samples normally fell within the 3.5−5.0 V interval and changed only weakly after doping, decreasing slightly (by $\sim$ 30%) at the maximum impurity concentration.

The fact that switching occurred at higher current values (Figure 2, *b*) in films with a Bi impurity concentration of 12.0 at% may be indicative of certain features of nucleation in these films associated with their higher crystal nucleating power and leading to a reduction in the film resistance upon switching.

Key parameters of CVCs of GST225 samples with different concentrations of the Bi impurity

| Sample № | Base electrode material | Polarity | Bi concentration, at% | $R_{in}$, kΩ | $R_{fin}$, Ω | $U_{th}$, V | $U_{hold}$, V | Oscillations |
|---|---|---|---|---|---|---|---|---|
| 1 | TiN | Forward | 0 | 334 | 328 | 3.5 | 0.62 | + |
| 1 | TiN | Reverse | 0 | 646 | 304 | 5.8 | | − |
| 2 | Al | Forward | 0 | 394 | 70 | 4.3 | | + |
| 2 | Al | Reverse | 0 | 561 | 39 | 5.2 | | + |
| 3 | TiN | Forward | 6.3 | 200 | 326 | 3.4 | 0.7 | − |
| 3 | TiN | Reverse | 6.3 | 227 | 417 | 4.1 | | − |
| 4 | Al | Forward | 6.3 | 384 | 866 | 5.0 | 0.6 | − |
| 4 | Al | Reverse | 6.3 | 350 | 36 | 4.8 | | − |
| 5 | TiN | Forward | 12 | 134 | 315 | 2.5 | 0.8 | − |
| 5 | TiN | Reverse | 12 | 33.4 | 684 | − | | − |
| 6 | Al | Forward | 12 | 25 | 111 | 2.9 | | − |
| 6 | Al | Reverse | 12 | 22 | 57 | 3.5 | | − |

The key results of the conducted experiments are presented in the table in the form of average values of quantities measured at different positions of the top electrode ($\geq 10$) on the CGS film surface. It is evident that the introduction of

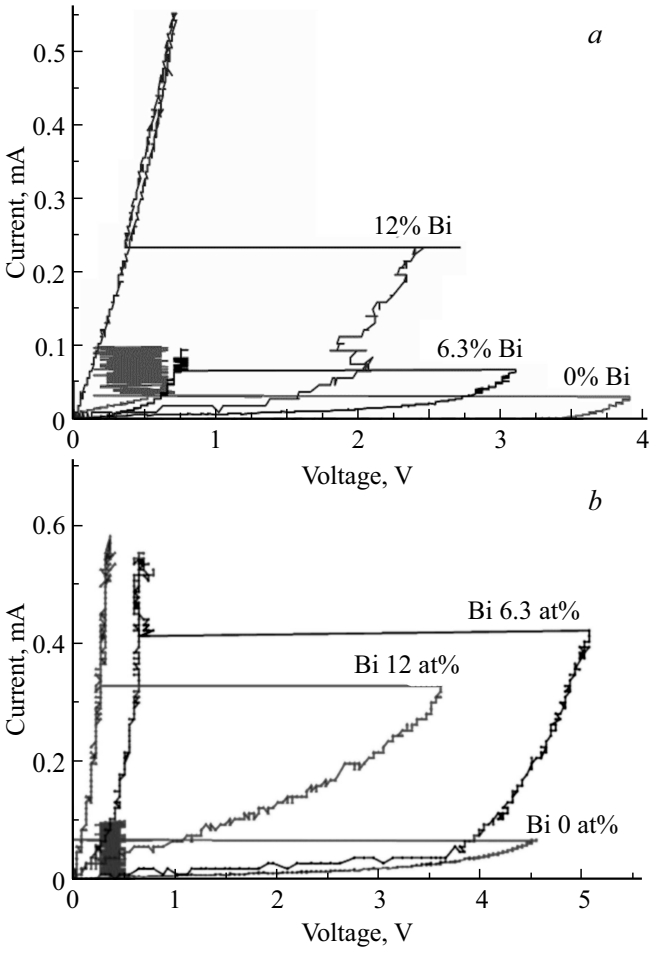


**Figure 2.** Typical CVCs of doped and undoped GST225 samples with switching effect and the base electrode made of TiN (*a*) and Al (*b*).

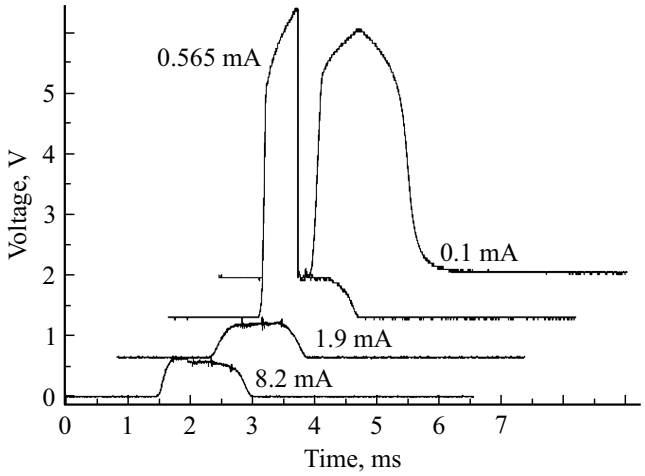


**Figure 3.** Oscilloscope records for GST225 samples doped with 6.3 at% Bi (base electrode — Al) exposed to a sequence of current pulses with increasing $I_{max}$. The curves corresponding to different current values are shifted along both axes for clarity.

Bi led to a reduction in initial resistance $R_{in}$ of the samples measured at low currents ($I_{max} = 6.5\,\mu$A): it decreased by a factor of 3 (15) at an impurity concentration of 12.0 at% for the sample with the TiN (Al) base electrode.

Final resistance $R_{fin}$ measured at current $I_{max} = 8.2$ mA and corresponding to the resistance of the sample in the crystalline state with memory was virtually independent of the impurity concentration. Notably, the $R_{fin}$ values for the sample with the TiN base electrode were significantly ($\sim 3$ times) higher than those corresponding to the Al electrode.

It can be seen from the table that the initial resistance increased by a factor of 1.5−2 when reverse-polarity voltage (minus at the top electrode) was applied to undoped samples. This suggests the presence of a contact potential difference. In doped samples, $R_{in}$ remained virtually unchanged after polarity reversal, but

$R_{fin}$ increased (decreased) if the base electrode was made of TiN (Al). These facts highlight the importance of the base electrode material and provide evidence of a contact potential difference.

Various mechanisms have been proposed in literature to explain the increase in electrical conductivity in doped CGSs [1,18,20,21]: an impurity may affect the density of both charged and neutral intrinsic defects, and the possibility of impurity conduction also cannot be excluded. In our view, the mechanism of defect „healing" is likely to be manifested, since the Bi impurity, being isomorphic to Sb, may act similarly to it and, interacting with the dangling chalcogen bond, form a strong chemical bond with Te in GST225.

## 4. Conclusion

An appreciable influence of Bi impurity on the CVC parameters was noted at the maximum impurity concentration (12.0 at%): switching voltage Uth decreased, $U_{hold}$ increased by $\sim 30\%$, and initial resistance $R_{in}$ of the samples decreased by a factor of 3−15. The introduction of Bi also resulted in complete suppression of voltage fluctuations after switching. The results of measurements with forward and reverse polarity are indicative of the presence of a contact potential difference.

The CVCs obtained for the studied samples with an impurity concentration of 12.0 at% have the following major features:

– an almost complete lack of a vertical section, which made it impossible to determine holding voltage $U_{hold}$;

– the reverse CVC branch measured with decreasing current applied to the sample was virtually coincident with the forward branch.

These facts suggest that crystallization occurs almost immediately after switching. As a result, the subsequent increase in current does not induce a change in the sample resistance. This CVC behavior may be attributed to a higher crystal nucleating power of doped samples.

The obtained results allow us to conclude that the stability of electrical properties of GST225 increases following the introduction of Bi by radio-frequency ion-plasma magnetron co-sputtering. These data may be used in the development of phase-change memory devices to improve their key parameters.

### Funding

This study was supported in part by grant No. AR14871061 from the Committee of Science of the Ministry of Science and Higher Education of the Republic of Kazakhstan.

### Conflict of interest

The authors declare that they have no conflict of interest.

## References

[1] N.A. Bogoslovskiy, K.D. Tsendin, Semiconductors, **46** (5), 559 (2012).
[2] S.A. Kozyukhin, P.I. Lazarenko, A.I. Popov, I.L. Eremenko. Russ. Chem. Rev., **91** (9), RCR5033 (2022).
[3] *Phase Change Memory. Device Physics, Reliability and Applications*, ed. by A. Redaelli (Springer Cham, 2018).
[4] N. Li, C. Mackin, A. Chen, K. Brew, T. Philip, A. Simon, I. Saraf, J.-P. Han, S.G. Sarwat, G.W. Burr, M. Rasch, A. Sebastian, V. Narayanan, N. Saulnier. Adv. Electron. Mater., **9** (6), 2370030 (2023).
[5] K. Zhao, W. Han, Z. Han, X. Zhang, X. Zhang, X. Duan, M. Wang, Y. Yuan, P. Zuoet. Nanophotonics, **11** (13), 3101 (2022).
[6] Zh. Tolepov, O. Prikhodko, A. Kolobov, G. Ismailova, S. Peshaya, N. Guseinov, Y. Mukhametkarimov, A. Kapanov, S. Maksimova. J. Non-Cryst. Sol., **642**, 123167 (2024).
[7] A. Sherchenkov, P. Lazarenko, A. Babich, D. Terekhov, S. Kozyukhin. *Int. Conf. Mechanics, Materials and Structural Engineering* (ICMMSE 2016).
[8] A. Babich, A. Sherchenkov, S. Kozyukhin, P. Lazarenko, O. Boytsova, A. Shuliatyev. J. Thermal Analysis and Calorimetry, **127** (1), 283 (2016).
[9] S. Kozyukhin, A. Sherchenkov, A. Babich, P. Lazarenko, H.P. Nguyen, O. Prikhodko. Canadian J. Phys., **92** (7/8), 684 (2014).
[10] M. Wuttig, H. Bhaskaran, T. Taubner. Nature Photonics, **11** (8), 465 (2017).
[11] B. Gholipour, S.R. Elliott, M.J. Müller, M. Wuttig, D.W. Hewak, B.E. Hayden, Y. Li, S.S. Jo, R. Jaramillo, R.E. Simpson, J. Tominaga, Y. Cui, A. Mandal, B.J. Eggleton, M. Rochette, M. Rezaei, I. Alamgir, H.M. Shamim, R. Kormokar, A. Anjum, G.T. Zeweldi, T.S. Karnik, J. Hu, S.O. Kasap, G. Belev, A. Reznik. J. Phys. Photonics, **5**, 012501 (2023).
[12] D.V. Christensen, R. Dittmann, B. Linares-Barranco, A. Sebastian, M. Le Gallo, A. Redaelli, S. Slesazeck, T. Mikolajick, S. Spiga, S. Menzel, I. Valov, G. Milano, C. Ricciardi, S.-J. Liang, F. Miao, M. Lanza, T.J. Quill, S.T. Keene, A. Salleo, J. Grollier, D. Marković, A. Mizrahi, P. Yao, J.J. Yang, G. Indiveri, J.P. Strachan, S. Datta, E. Vianello, A. Valentian, J. Feldmann, X. Li, W. HP Pernice, H. Bhaskaran, S. Furber, E. Neftci, F. Scherr, W. Maass, S. Ramaswamy, J. Tapson, P. Panda, Y. Kim, G. Tanaka, S. Thorpe, C. Bartolozzi, T.A. Cleland, C. Posch, S. Liu, G. Panuccio, M. Mahmud, A.N. Mazumder, M. Hosseini, T. Mohsenin, E. Donati, S. Tolu, R. Galeazzi, M.E. Christensen, S. Holm, D. Ielmini, N. Pryds. Neuromorph. Comput. Eng., **2**, 022501 (2022).
[13] F. Brückerhoff-Plückelmann, J. Feldmann, C.D. Wright, H. Bhaskaran, W.H.P. Pernice. J. Appl. Phys., **129**, 151103 (2021).
[14] P. Narayanan, S. Ambrogio, A. Okazaki, K. Hosokawa, H. Tsai, A. Nomura, T. Yasuda, C. Mackin, S.C. Lewis, A. Friz, M. Ishii, Y. Kohda, H. Mori, K. Spoon, R. Khaddam-Aljameh, N. Saulnier, M. Bergendahl, J. Demarest, K.W. Brew, V. Chan, S. Choi, I. Ok, I. Ahsan, F.L. Lie, W. Haensch, V. Narayanan, G.W. Burr. IEEE Trans. Electron Dev., **68** (12), 6629 (2021).
[15] S.A. Fefelov, L.P. Kazakova, S.A. Kozyukhin, K.D. Tsendin, D. Arsova, V. Pamukchieva. Tech. Phys., **59** (4), 546 (2014).

[16] S.A. Fefelov, L.P. Kazakova, D. Arsova, S.A. Kozyukhin, K.D. Tsendin, O.Yu. Prikhodko. Semiconductors, **50** (7), 941 (2016).
[17] S.A. Fefelov, L.P. Kazakova, N.A. Bogoslovskiy, K.D. Tsendin. Semiconductors, **52** (12), 1607 (2018).
[18] *Elektronnye yavleniya v khal'kogenidnykh stekloobraznykh poluprovodnikakh*, Ed. by K.D. Tsendin (SPb., Nauka, 1996). (in Russian).
[19] N. Bogoslovskiy, K. Tsendin. Solid-State Electron., **129**, 10 (2017).
[20] N.F. Mott, E.A. Davis. *Electronic Processes in Non-Crystalline Materials* (Clarendon Press, 1979).
[21] *Phase Change Materials Science and Applications*, ed. by S. Raoux and M. Wuttig (N.Y., Springer, 2009).

*Translated by D.Safin*